



Phytoplankton composition in Mediterranean confined coastal lagoons: testing the use of ecosystem metabolism for the quantification of community-related variables

Maria Bas-Silvestre¹ · Maria Antón-Pardo^{1,4} · Dani Boix¹ · Stéphanie Gascón¹ · Jordi Compte¹ · Jordi Bou² · Biel Obrador³ · Xavier D. Quintana¹

Received: 15 October 2023 / Accepted: 3 May 2024

© The Author(s) 2024

Abstract

Estimations of ecosystem metabolism have rarely been used to quantify productivity in structural reductionist approaches for the description of phytoplankton composition. However, estimations of ecosystem metabolism could contribute to a better understanding of the relationship between phytoplankton composition and ecosystem functioning. To examine this, we investigated the community structure of phytoplankton in a set of Mediterranean coastal lagoons (natural and artificial) during a hydrological cycle to identify the most important environmental variables determining phytoplankton species composition. The focus of the study was on the quantification of productivity-related variables using estimations of ecosystem metabolism, such as different proxies for the estimation of the production-to-biomass ratio and of the relative importance of *K*- and *r*-strategies, which are commonly used conceptually but not quantified. Our results demonstrated differences in phytoplankton composition between seasons, due to the dominant hydrological pattern of flooding confinement in the salt marsh, and between lagoons that were caused by different levels of nutrient availability. Moreover, there was a notable decrease in the production/biomass ratio and a prevalence of *K*-strategists with seasonal succession, as predicted by Margalef's mandala. Thus, the results showed that estimations of ecosystem metabolism are useful for the higher frequency quantification of important ecological variables, and contribute to a better understanding of planktonic assemblages, and physical and chemical changes, in these fluctuating ecosystems.

Keywords Coastal lagoons · Phytoplankton community · Margalef's mandala · Metabolic rates · Production/biomass ratio · *K*-strategy · *r*-strategy

Introduction

In 1978, Ramon Margalef (1978) published a conceptual two-dimensional model, 'Margalef's mandala', to explain the influence of physical and nutritional forces on phytoplankton life-form succession. In that tentative plot (Fig. 1) a main distinction was made between the replacement of organisms able to grow in nutrient-rich, turbulent environments (termed *r*-strategists, e.g. diatoms) and those able to grow under low nutrient concentrations and low turbulence (*K*-strategists, e.g. dinoflagellates). Through this work, Margalef introduced the now familiar concept of functional groups and the use of trait-based models to predict phytoplankton community composition (Litchman and Klausmeier 2008). Margalef's mandala has since been expanded and refined for different aquatic systems and organisms (Cullen et al. 2002, 2007; Balch 2004), including coastal lagoons

✉ Maria Bas-Silvestre
maria.bas@udg.edu

¹ Grup de Recerca en Ecologia Aquàtica Continental (GRECO), Institute of Aquatic Ecology, Facultat de Ciències, University of Girona, Carrer Maria Aurèlia Capmany, 69, 17003 Girona, Spain

² LAGP-Flora and Vegetation, Institute of the Environment, Facultat de Ciències, University of Girona, Carrer Maria Aurèlia Capmany, 69, 17003 Girona, Spain

³ Departament de Biologia Evolutiva, Ecologia i Ciències Ambientals. Institut de Recerca de la Biodiversitat (IRBio), Universitat de Barcelona, 08028 Barcelona, Spain

⁴ Present Address: Institut Cavanilles de Biodiversitat i Biologia Evolutiva, Universitat de València, C/ Catedràtic José Beltrán Martínez 2, 46980 Paterna (València), Spain

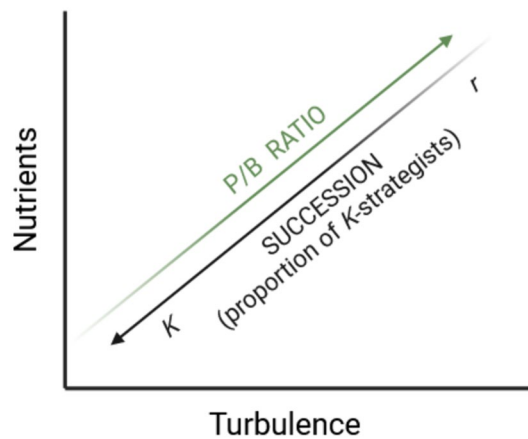


Fig. 1 Simplified scheme of Ramon Margalef's (1978) mandala, in which phytoplankton responses to turbulence and nutrients are shown in black. The expected relationship between production and biomass [production/biomass ratio (*P/B RATIO*)] with succession is represented in green (color figure online)

(Glibert 2016; Derolez et al. 2020), where phytoplankton constitutes an important biological indicator (Seoane et al. 2011; Hemraj et al. 2017; Leruste et al. 2018). In fact, elucidating the drivers that regulate the community assembly and dynamics of phytoplankton continues to be of great importance to understanding the ecology of coastal lagoons (Péquin et al. 2017; Pulina et al. 2018; Villamaña et al. 2019; Derolez et al. 2020).

Despite its associated uncertainties productivity is one of the most important factors in Margalef's mandala, it has rarely been quantified in studies dealing with phytoplankton community structure, and has generally only been considered in a theoretical context. Furthermore, ecosystem metabolism has gained importance for the analysis of aquatic ecosystem functioning (Staeher et al. 2012; Hoellein et al. 2013), and has been estimated using a wide range of methods (Kemp and Testa 2011). One of the most popular methods relies on measuring diel free-water dissolved oxygen (DO) dynamics (Odum 1956), which has become a generalized method because of its simplicity and use of reliable and affordable sensor technologies. Despite its associated uncertainties and being based on several assumptions, this diel free-water DO method is considered an excellent monitoring tool for studying ecosystem functioning (Staeher et al. 2010, 2012). However, although widely used in holistic functional studies, estimations of ecosystem metabolism have rarely been used to quantify productivity in structural reductionist approaches for the description of phytoplankton composition [but see Duarte et al. (2006) and Zwart et al. (2015)]. Moreover, the modelling techniques used in metabolism estimations, such as those based on a Bayesian approach (Grace et al. 2015), decompose metabolic rates into several parameters obtained from photosynthesis-irradiance (P-I) curves, and provide

some variables that, again under several assumptions, may be related to growth rate or carrying capacity, which are two parameters of great importance to evaluating the relative importance of *r*- or *K*-strategists in a phytoplankton community. Bearing all of this in mind, ecosystem metabolism measurements can potentially contribute to a better understanding of the relationship between phytoplankton composition and ecosystem functioning, through the quantification of ecologically meaningful variables that are also useful for the development of management and conservation strategies for aquatic systems.

Coastal lagoons are productive and highly dynamic transitional water bodies. Their ecosystem functioning and productivity are influenced by strong fluctuations in biological, hydrological, physical and chemical characteristics (Kennish and Paerl 2010; Pérez-Ruzafa et al. 2019). Therefore, there is increasing interest in deepening our understanding of these characteristics due to the particular vulnerability of coastal lagoons to global change (Kennish and Paerl 2010; Brito et al. 2012; Saccà 2016) and how phytoplankton communities will adapt to these changes. Moreover, because of their high level of degradation, especially in the Mediterranean region, coastal lagoons are included in the Habitats Directive of the European Commission as priority habitats (Council Directive 92/43/EEC), and several restoration efforts have been developed to try to recover their ecological value and their ecosystem services (Quintana et al. 2018). In Mediterranean coastal lagoons metabolic variation and physical changes occur at high rates (Saccà 2016; Bas-Silvestre et al. 2020), and some restoration efforts have shown that nutrient availability differs between newly created and existing lagoons (Badosa et al. 2006; López-Flores et al. 2006a; Quintana et al. 2018). Strong variations in both metabolic rates and nutrient availabilities make these ecosystems especially suitable for the combined analysis of community structure and ecosystem functioning, as they exist under a wide range of conditions.

We analysed the phytoplankton community structure and measured environmental variables in a set of Mediterranean coastal lagoons to identify the most important variables determining the species composition of this community. We chose to examine the confined coastal lagoons located in La Pletera salt marsh, where a restoration program has been developed to recover the ecological functioning of the whole salt marsh, and where there are both natural and artificial lagoons that experience the same hydrological conditions. We simultaneously took measurements in the lagoons to estimate metabolic rates to show the relationship between these and species composition and, in this regard, to emphasize the quantification of productivity-related variables that are related to ecosystem metabolism and are of ecological significance. We expected the productivity-related variables associated with ecosystem metabolism to represent

high-frequency estimators for the determination of species composition, as indicated by the main dimensions in Margalef's mandala.

Materials and methods

Study site

The study was undertaken in six permanent water bodies located in the protected salt marsh of La Pletera, in the Baix Ter wetlands (Estartit, Girona, Spain) (Fig. 2). These water bodies are defined as confined coastal brackish or hyperhaline lagoons (Trobajo et al. 2002), with no continuous surface freshwater or seawater inflow. Surface water exchange in these water bodies generally occurs during unpredictable sea storms or intense rainfall events, after which groundwater flow, which accounts for 80% of their water exchange, increases (Menció et al. 2017; Quintana et al. 2018). During

the summer months, the water level decreases and salinity increases. Thus, there is a dominant hydrological pattern of flooding-confinement, with strong fluctuations in water level and salinity, which drives the different dynamics of organic matter, nutrients, species composition and ecosystem metabolism (Badosa et al. 2006; Quintana et al. 2018, 2021; Cabrera et al. 2019; Bas-Silvestre et al. 2020). Despite the general hydrological features of the salt marsh, these lagoons differ in some characteristics (Table 1), which partially depend on their different origins. In the 1980s, La Pletera salt marsh suffered partial urbanisation, with alterations to the landscape, although two natural water bodies (FRA and BPI) remained. Some years later, new lagoons (G02, L01, L04 and M03), surrounded by the salt marsh vegetation, were created during two different LIFE Nature restoration projects with the aim of restoring the ecological functioning of the area (Quintana et al. 2018). G02 was created in 2002 during the first (LIFE99 NAT/E/006386), and L01, L04 and M03 during the second LIFE Project (LIFE13 NAT/ES/001001) in 2016 (Fig. 2). More information on these restoration actions can be found at www.lifepletera.com.

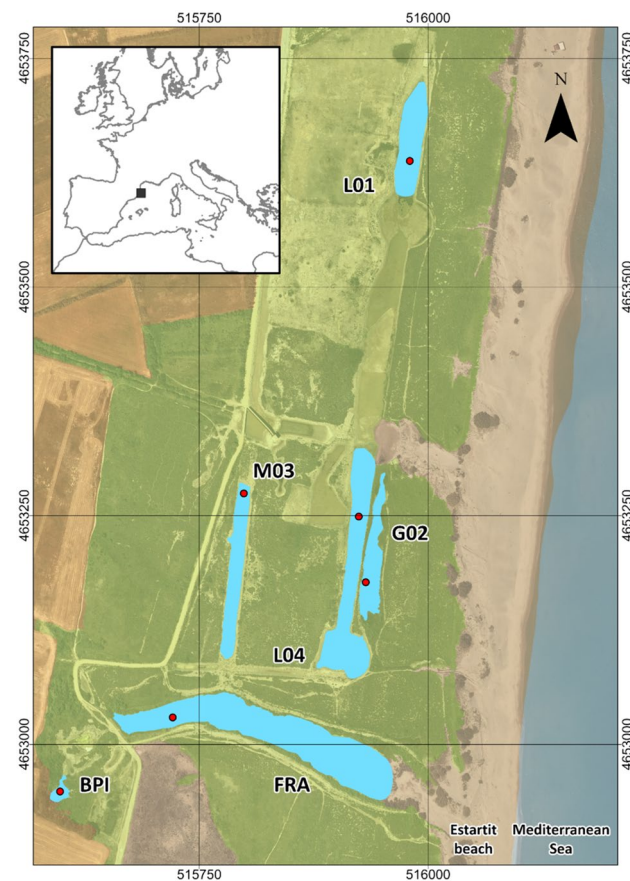


Fig. 2 Location of the six Mediterranean confined coastal lagoons studied (in blue) in La Pletera salt marsh (Girona, northeastern Iberian Peninsula) (inset). Areas in green correspond to salt marsh vegetation, while those in brown indicate extensive agriculture. Red dots indicate the location of the high-frequency monitoring probes (color figure online)

Sampling procedure and water analyses

The study was conducted during a complete hydrological cycle from July 2018 to August 2019 in the six confined lagoons of La Pletera salt marsh (Fig. 2; Table 1). Ten-litre integrated water samples were collected monthly from at least eight points in each lagoon at a depth between 5 and 80 cm. The nutrient and plankton samples were obtained from this integrated volume. Water samples for inorganic nutrient analyses were filtered in the field through precombusted (450 °C for 4 h) Whatman GF/F filters (0.7- μ m pore) and frozen until analysis. Ammonium (NH_4^+), nitrite (NO_2^-) and nitrate (NO_3^-) were analysed following American Public Health Association (APHA) (2005), and phosphate (PO_4^{3-}) was measured according to UNE-EN-ISO6878. Unfiltered water samples for the analysis of total nitrogen (TN), total phosphorus (TP) and total organic carbon (TOC) were also taken. TOC and TN were measured using a TOC analyser (TOC-V CSH SHIMADZU). The TP analyses were performed as described by Grasshoff et al. (1999). Organic forms of nitrogen (N_{org}) and phosphorus (P_{org}) were calculated as the difference between TN or TP and the sum of their inorganic forms. Dissolved inorganic nitrogen (DIN) was calculated as the sum of NH_4^+ , NO_2^- , and NO_3^- . pH and gilvin (coloured, dissolved organic matter) levels were also recorded. Gilvin was measured from filtered water samples, according to Kirk (1994), as the absorbance at 440 nm, by using a spectrophotometer (Shimadzu UV-1800). Seagrass and macroalgae cover (Table 1) were calculated using geographic information systems (GIS) software together with

Table 1 Mean value and range (*in parentheses*) of physical and chemical variables measured in the surface waters of six lagoons in La Pletera during the study period (July 2018 to August 2019)

	BPI	FRA	G02	L01	L04	M03
Water temperature (°C)	20.0 (2.3–34.6)	19.7 (1.8–35.4)	19.2 (1.1–35.3)	19.3 (1.6–33.8)	18.6 (1.9–33.3)	20.1 (2.4–35.8)
Salinity (‰)	53.3 (10.7–90.5)	45.3 (26.5–73.7)	25.6 (7.7–52.7)	15.4 (5.3–25.7)	23.5 (6.1–40.2)	48.0 (10.2–90.5)
pH	8.6 (8.2–9.0)	8.4 (7.9–8.8)	8.8 (8.2–9.8)	8.7 (8.0–9.6)	9.1 (8.4–9.8)	8.7 (8.0–9.7)
Chlorophyll <i>a</i> (µg L ⁻¹)	98.9 (2.5–310.2)	71.4 (1.9–250.4)	38.5 (1.1–236.6)	0.7 (0.0–1.9)	13.1 (0.7–45.4)	6.4 (0.0–29.6)
DIN (mg N L ⁻¹)	0.30 (0.02–1.36)	0.40 (0.10–2.33)	0.15 (0.04–0.60)	0.92 (0.05–6.29)	0.09 (0.02–0.19)	0.16 (0.04–0.45)
PO ₄ ³⁻ (mg P L ⁻¹)	0.05 (0.00–0.17)	0.04 (0.01–0.15)	0.04 (0.00–0.09)	0.01 (0.00–0.02)	0.02 (0.00–0.04)	0.04 (0.00–0.33)
N _{org.} (mg L ⁻¹)	12.24 (2.89–30.23)	5.64 (2.33–13.19)	4.12 (1.29–10.89)	1.89 (0.54–3.28)	2.45 (1.10–4.49)	4.28 (1.92–7.65)
P _{org.} (mg L ⁻¹)	0.32 (0.08–0.63)	0.24 (0.03–0.70)	0.15 (0.01–0.41)	0.02 (0.00–0.08)	0.07 (0.01–0.20)	0.10 (0.01–0.44)
TN (mg L ⁻¹)	12.54 (3.06–30.31)	6.03 (2.61–13.51)	4.27 (1.33–11.19)	2.81 (1.49–8.89)	2.54 (1.19–4.62)	4.44 (2.03–8.11)
TP (mg L ⁻¹)	0.32 (0.02–0.64)	0.27 (0.05–0.86)	0.18 (0.02–0.45)	0.03 (0.01–0.10)	0.09 (0.01–0.23)	0.13 (0.01–0.77)
TOC (mg L ⁻¹)	127.89 (29.9–265.6)	45.48 (25.82–104.5)	36.70 (14.81–73.89)	16.98 (10.12–35.03)	22.10 (11.00–34.31)	30.62 (11.00–68.51)
Depth (m)	0.7 (0.4–1.1)	1.6 (1.4–2.1)	0.9 (0.6–1.4)	0.5 (0.4–1.0)	0.7 (0.5–1.2)	0.6 (0.3–1.1)
Surface (m ²) ^a	195	10326	2240	3345	5157	1905
Seagrass cover (%) ^b	0, 0, 0, 0	0, 0, 0, 0	0, 41, 27, 46	14, 10, 13, 85	66, 88, 30, 89	0, 0, 0, 0
Macroalgae cover (%) ^b	0, 0, 16, 5	4, 2, 27, 17	0, 0, 0, 5	0, 2, 0, 6	10, 0, 15, 8	80, 84, 65, 27

DIN Dissolved inorganic nitrogen, N_{org.} organic nitrogen, P_{org.} organic phosphorus, TN total nitrogen, TP total phosphorus, TOC total organic carbon

^aSurface area values correspond to the mean level of the lagoons

^bValues were recorded on 18 October, 18 December, 19 May, and 19 August, respectively

orthophotographs, from which digital maps were created. All cartographic information was managed using the ESRI ArcGIS Pro programme (Esri, 2020). Aerial photographs were taken seasonally during the study period (18 October, 18 December, 19 May, and 19 August). As monthly data were not available, these data were only used for lagoon characterization.

High-frequency monitoring and metabolism estimations

Continuous, high-frequency monitoring of different physical variables was needed for the metabolism calculations. Optical DO sensors (MiniDOT; PME, USA) and conductivity loggers (CTD-divers; VanEssen Instruments, the Netherlands) were deployed 30 cm from the surface at the deepest and most representative point of each lagoon to obtain DO, temperature and conductivity measurements every 10 min. The conversion of conductivity to salinity was performed according to APHA (2005). Wind speed and photosynthetically active radiation were measured at the same frequency in the salt marsh using a Kestrel-5000 Environmental Meter (Kestrel Instruments, USA) and

HOBO pendant (Onset, USA) data logger, respectively. All of the lagoons, with the exception of FRA (during winter), were usually well mixed, and Z_{mix} was equal to the water level that was recorded in each lagoon using high-frequency loggers (CERA-Diver; VanEssen Instruments). During the winter months, Z_{mix} in FRA was calculated every 10–15 days from density profiles, as described in Bas-Silvestre et al. (2020).

Gross primary production (GPP) and ecosystem respiration (ER) were estimated using a modified version of the BAYesian Single-station Estimation (BASE) program (Grace et al. 2015; Bas-Silvestre et al. 2020). To avoid temperature effects, metabolic rates were determined from ER standardized to 20 °C (ER₂₀); GPP was also standardized, to maximum light conditions (GPP_{MAX}) and to maximum light conditions at 20 °C (GPP_{20MAX}). Thus, GPP_{20MAX} was obtained to represent the capacity for production, i.e. the maximum production of autotrophs at 20 °C if light were unlimited. For more details on model functioning, day validation and the parameter calculation procedure, see Bas-Silvestre et al. (2020). As phytoplankton samples were collected monthly, we calculated the monthly median value from the daily metabolic rates.

Flow cytometry and high-performance liquid chromatography analysis

Flow cytometry (FCM) was used to calculate the abundance and biovolume of nanoplankton (3–20 μm) and picoplankton (< 3 μm). We identified the different nano- and picoplankton groups according to their position in the FCM plots, i.e. according to their body size and fluorescence signal; the main blooms were also verified by microscopy. Of note is that different species that did not differ substantially in body size and pigment content were observed in the same FCM region. Thus, the different groups identified do not actually represent species, but ‘functional groups’, which we will refer to here ‘phytoplankton groups’, based on the assumption that species with similar body sizes and similar pigment contents have a similar functional role in an aquatic ecosystem (Table 2). Samples of lagoon water filtered through a 50- μm mesh were fixed by adding 0.5 mL of paraformaldehyde (1%)-glutaraldehyde (0.05%) to a total volume of 4.5 mL for FCM, following Gasol and Morán (2015). The entire procedure used is described in López-Flores et al. (2009). Beads were used as internal standards, and all parameters were normalized to these. Data were analysed using BD CellQuest Pro software. As side scatter in FCM is related not only to the internal structure of the organisms but also to cell size [Gasol and Morán (2015) and references therein], we estimated cell volumes from side scatter signals using a calibration curve. Different cultures of known phytoplankton species were run on the flow cytometer, and a linear regression was performed between the average side scatter value of the phytoplankton population, normalized to that of the beads, and the population mean volume obtained by inverted microscopy, similarly to López-Flores et al. (2009) and references therein.

To help identify dominant nano- and picoplankton species forming blooms, an analysis of pigments was also conducted. We used several diagnostic pigments to identify certain taxonomic groups, following Jeffrey et al. (1997); chlorophyll *a* was used to estimate primary producer biomass. Samples were analysed using a high-performance liquid chromatography (HPLC) method with a reverse-phase C_8 column and pyridine-containing mobile phases (Zapata et al. 2000; López-Flores et al. 2006a). A Waters high-performance liquid chromatography system with a Waters 996 Photodiode Array Detector was used. Chlorophylls and carotenoids were detected by diode array spectroscopy (350–700 nm). The pigments detected when groups bloomed are listed in Table 2.

Phytoplankton and zooplankton counting using inverted microscopy

To estimate the abundance and biovolume of microphytoplankton (> 20 μm), which are poorly estimated by FCM

or are even excluded from the FCM counting procedure (> 50 μm), we used a Zeiss Axio VertA1 inverted microscope. A 125-mL volume of unfiltered sampled water was fixed with formaldehyde (10% final concentration) in an amber glass bottle. An inverted microscope was used to identify and measure the cells of a 30-mL subsample after sedimentation for at least 10 h, in accordance with Utermöhl (1958). At least 100 individuals were counted or 20 fields at $\times 400$ magnification (40x objective and 10x ocular lenses) were used for counting for abundance estimations; for rare, bigger specimens (> 50 μm) one-quarter, one-half or the whole sample was examined at $\times 100$ magnifications (10x objective and 10x ocular lenses). Measurements of linear dimensions of the cells (25 individuals per group) were used to estimate the biovolume from geometric formulae (Hillebrand et al. 1999). Although some organisms were identified to the genus or species level, for statistical analyses, phytoplankton cells were classified into the major algal divisions or classes. Classifying the phytoplankton in this way enables the determination of homogeneous groups that are comparable to nano- and picoplankton groups counted by FCM. Where different species from the same group were identified by microscopy, we added ‘large’ to the group abbreviation (see Table 2). We added ‘high’ or ‘low’ to the group abbreviations to reflect the FL3 signal. Microplankton smaller than 20 μm , when identifiable, were counted by microscopy ensuring that they were not counted by FCM.

The abundance and biovolume of small ciliates (< 50 μm) was also estimated using the microphytoplankton counts described above and using the same Hillebrand et al. (1999) formulae for biovolume estimations. Zooplankton (> 50 μm) samples were obtained by filtering a total volume of 5 L through a 50- μm mesh and fixed in situ in 4% formalin. Identification and counting of the different taxa were performed to the lowest taxonomic level without specimen manipulation under an inverted microscope. For each taxon found in the 50- μm counts, we measured 25 individuals to estimate the organisms’ body size and biomass (dry weight). See Cabrera et al. (2019) for more details on zooplankton processing and biomass estimations. We distinguished between detritivores or non-selective bacterivorous filter feeders (e.g. harpacticoid copepods or rotifers with a malleate or ramate mastax) (Nogrady 1993) and selective filter-feeding algivores or predators (e.g. rotifers with a virgate or incudate mastax or calanoid and cyclopid copepods) (Einsle 1993).

Data analysis

Drivers of phytoplankton composition

Factors determining phytoplankton composition were evaluated by redundancy analysis (RDA) where the significant

Table 2 Main features of the phytoplankton groups identified during the present study by microscopy and flow cytometry together with high-performance liquid chromatography

Phytoplankton group	Size classification	ESD ^a (µm)	FL2	FL3	Pigment(s) detected when blooming	Typical representative (s)	Reynolds functional groups	Potential phagotrophy	Flagella	Potential toxicity	Abbreviation
Euglenophytes	Microplankton	21.1 (1.9)	–	–	–	<i>Euglena</i>	W1	No	Yes	No	EUGLE
Dinoflagellates	Microplankton	21.5 (8.1)	–	–	Peridinin	<i>Oxyrrhis marina</i> , <i>Glenodinium</i> , <i>Gymnodinium</i> , <i>Scipistella</i>	Y	Yes	Yes	Yes	DINO
Diatoms	Microplankton	17.3 (5.0)	–	–	Fucoxanthin	<i>Nitzschia</i> , <i>Navicula</i> , <i>Cyclotella</i> , <i>Gyrosigma</i> , <i>Achnanthes</i>	D	No	No	No	DIATlarge
Cyanobacteria	Microplankton	21.0 (9.1)	–	–	–	<i>Anabaena</i> , <i>Oscillatoria</i>	H1, T _C	No	No	Yes	CYANlarge
Prasinophytes	Microplankton	16.3 (2.5)	–	–	Chlorophyll <i>b</i> , lutein	<i>Pyramimonas</i>	X2	No	Yes	No	PRASlarge
Cryptophytes	Nanoplankton	15.0 (4.0)	High	High	Alloxanthin	<i>Hemiselmis</i> , <i>Chroomonas</i>	X2	Yes	Yes	No	CRYPTO
Haptophytes	Nanoplankton	9.4 (3.1)	Low	Low	Fucoxanthin, 19'-hex- anoyloxyfucoxanthin	<i>Pavlova</i> -like cells	X2	Yes	Yes	Yes	HAPTlow
Diatoms/Prasinophytes	Nanoplankton	5.7 (1.4)	Low	High	Fucoxanthin	<i>Nitzschia closterium</i> , <i>Cyclotella</i> , <i>Pyramimonas</i>	D, X2	No	No ^b	No	AUTOhigh
Haptophytes	Nanoplankton	5.0 (2.1)	Low	High	Fucoxanthin, 19'-hex- anoyloxyfucoxanthin	<i>Prymnesium</i> -like cells	X2	Yes	Yes	Yes	HAPThigh
Photosynthetic bacteria	Picoplankton	3.5 (1.1)	Low	Low	–	<i>Chromatium</i>	V	No	Yes ^b	No	PHOTOB
Picoeukaryotes	Picoplankton	1.9 (0.5)	Medium	High	Chlorophyll <i>b</i> , lutein	<i>Nannochloris</i> -like cells	K	No	No	No	PICOEUK
Cyanobacteria	Picoplankton	1.9 (1.2)	High	Low	–	<i>Synechococcus</i> -like cells	K	No	No	Yes	SYNEC

Classification of phytoplankton groups in accordance with Reynolds functional groups was performed following Padisák et al. (2009) and according to the last changes summarised by Kruk et al. (2020)

ESD Equivalent spherical diameter, FL2 orange fluorescence signal, FL3 red fluorescence signal, large identified by microscopy, high or low in abbreviations refer to FL3 signal

^aMean and SD (in parentheses)

^bIndicates that the corresponding group was composed of different organisms, which did not have the same characteristics; therefore, it should be noted that the attribution of flagella (motility) was based on the most abundant organisms

variables were selected using a forward selection procedure. Abundances of the different phytoplankton groups (biovolume units) listed in Table 2 were used to build the RDA species matrix. Hellinger transformation was applied to the phytoplankton community data prior to analysis (Legendre and Gallagher 2001).

We based the analyses on the variables used by Glibert (2016) in her revisit of Margalef's mandala. Thus, as explanatory variables we used physical and chemical variables, nutrient and organic matter concentrations, top-down

control ratios (such as the ratio between phytoplankton and zooplankton biomass and the ratio between algivorous and bacterivorous zooplankton) and some other properties of the phytoplankton community (detailed in Table 3). These latter phytoplankton properties, including toxicity, phagotrophy and motility, were calculated by assigning each to the different phytoplankton groups (see Table 2) based on the literature (Reynolds 2006; Flynn et al. 2013; Jakubowska and Szelaq-Wasielewska 2015; Stoecker et al. 2017). For the phytoplankton/zooplankton biomass ratio (Table 3), their

Table 3 Summary of the different variables quantified in the present study and included in the redundancy analysis (RDA)

Type of variable	Variable	Abbreviation	Group ^b
Physical and chemical ^a	Temperature	<i>Temp</i>	1
	Salinity		1
	pH		1
	Depth		1
	Gilvin		1
	Daily variance in DO (%)	DOsat_var	1
Nutrients and organic matter	P _{org} /PO ₄ ³⁻	orgP_inorP	1
	N _{org} /DIN	orgN_inorN	1
	NH ₄ ⁺ /NO ₃ ⁻	redN_oxN	1
	DIN/PO ₄ ³⁻	N_P	2
	TOC/TP	TOC_TP	1
	TOC/TN	TOC_TN	1
	DIN		2
	PO ₄ ³⁻		2
	N _{org}		2
	P _{org}		2
TOC		2	
Top-down control	Algivorous/bacterivorous zooplankton	alg_bact	1
	Phytoplankton/zooplankton biomass	phyto_zoo	2
Phytoplankton properties	Cell size		2
	Motility		2
	Toxicity		2
	Phagotrophy		2
Productivity-related variables	Gross Primary Production	GPP	2
	Ecosystem Respiration	ER	2
	GPP standardized to 20 °C and maximum light	GPP _{20MAX}	2
	ER standardized to 20 °C	ER ₂₀	2
	ER/TOC	ER_TOC	2
	GPP/chlorophyll <i>a</i>	GPP_chla	2
	GPP _{MAX} (GPP standardized to maximum light)/A (primary production per quantum of light)	GPP _{MAX} _A	2

All variables and ratios listed in this table were log-transformed before statistical analysis to avoid spurious correlations (Pawłowsky-Glahn and Buccianti 2011). For more details on some of the calculations and analyses, see section "Materials and methods"

GPP Gross primary production, *ER* ecosystem respiration; for other abbreviations, see Table 1

^aExcluding nutrient contents

^bA major distinction was made between the variables included in the RDA (group 1) and those included in the RDA only as supplementary variables (group 2). The inclusion of variables as supplementary was for collinearity- or community-related reasons (see section "Data analyses")

biomasses were transformed to carbon units in accordance with Gaedke (1992). Some of the explanatory variables were not included in the original RDA (group 2 in Table 3) for the following reasons: (1) to avoid collinearity with other selected variables, whereby variables with an inflation factor > 10 in a forward selection procedure were discarded; (2) to avoid circularity, whereby those phytoplankton data obtained from some combinations of the relative abundances (biovolume units) of the different phytoplankton groups that were already included in the RDA species matrix were discarded.

All discarded variables (group 2 in Table 3) were later added as supplementary variables, which had no influence on the RDA, but helped to enhance the interpretability of the results. We also used categorical variables such as lagoon and season for classification and visualization. Monthly samples were assigned to one of two different seasons: summer (May–September) and winter (October–April). All individual variables and ratios listed in Table 3 were log-transformed before statistical analysis to avoid spurious correlations (Pawlowsky-Glahn and Buccianti 2011). Spearman correlations were computed to analyse the relationships between the different variables included in the study. The level of significance for all analyses was $p < 0.05$, (95% confidence interval). Statistical analyses and plots were achieved by using the *vegan* and *ggplot2* packages in R software (Wickham 2016; R Core Team 2017; Oksanen et al. 2019).

Productivity-related variables

To examine the relationships between metabolism and community structure, several variables related to metabolic rates and derived variables were only included in the RDA as supplementary variables (Group 2 in Table 3). As mentioned above, we did not include these variables as explanatory variables in the main RDA analysis to avoid forcing correlations between them and other variables, since our aim was to examine if there were relationships between metabolism and the main factors determining community structure. Metabolic rates were determined from measurements of GPP and ER, as well as the standardized rates of ER at 20 °C (ER_{20}) and GPP at 20 °C with no light limitation (GPP_{20MAX}) (Giling et al. 2017). The log-ratio between GPP and chlorophyll *a* was used as a proxy for the production/biomass ratio. Finally, the log-ratio between the GPP standardized to maximum light (GPP_{MAX}) and primary production per quantum of light (*A*) (GPP_{MAX}/A ratio) was used as a proxy for *K*- and *r*-strategies, for which a more detailed explanation is provided below. The BASE model used in this study estimates GPP on a daily basis by means of regressions between GPP and solar irradiation arriving at the lagoon surface, measured by using a typical P-I curve (Grace et al. 2015). The model outputs include not only daily GPP values

but also ecophysiological parameters with relevant ecological meaning. One of these parameters is *A*, which indicates primary production per unit light (i.e. photosynthetic efficiency) and under a growth curve model can be considered proportional to the growth rate (*r*) (Cullen 1990; Zonneveld 1998; Litchman and Klausmeier 2008). Moreover, GPP_{MAX} , which is obtained from the standardization of GPP to maximum light, can be considered to represent the carrying capacity (*K*) of a typical growth model. Thus, we propose that the log-ratio between these two parameters can be used as a proxy to quantify the *K*-*r* axis for the ecosystem studied.

Results

The two main axes of the RDA analysis accounted for 26.62% of the variation in phytoplankton composition (Fig. 3). The dynamics of the physicochemical variables during the study period support the differences between seasons as revealed by the RDA results (Figs. S2, S3). Thus, the first axis (RDA1) is related to seasonal physical changes and reflects the flooding-confinement pattern present in this type of salt marsh. Typical summer confinement conditions appear as negative values on RDA1 (Figs. 3, S1), with higher values for salinity, temperature and gilvin, and lower values for pH and the ratio of top-down grazing by algivorous and bacterivorous zooplankton (*alg_bact*; Table 3). Whereas winter flooding conditions were characterised by the opposite magnitude of these variables, and thus opposite coordinates in RDA1 (Figs. 3, S1). Lagoons BPI, FRA and M03 had the highest salinities and L01, L04 and G02 the lowest (Table 1; Fig. S2). During the hottest period of the study, which coincided with fewer days with rain and other sources of water input, the water levels decreased (Fig. S2). This decrease resulted in an increase in the concentrations of nutrients, organic matter (Fig. S3) and chlorophyll *a*.

Salinity, temperature and gilvin were the most significant variables that were negatively related to RDA1, while a major proportion of the algivorous zooplankton observed during winter conditions had a significant positive relationship with RDA1. Although these results were not statistically significant, under confinement conditions, *orgP_inorP*, *orgN_inorN* and *redN_oxN* were higher and *TOC/TP* was lower (Figs. S1, S4). Moreover, during the dry period, there was greater variability in *DO* (*DOsat_var*), which resulted in higher and greater variation in metabolic rates (Figs. S1, S5). Those values that indicated oversaturation were accompanied by extended periods of anoxia, especially in BPI, FRA and M03.

The second axis (RDA2) ordered the samples according to their origin, i.e. natural lagoons (positive values) and artificial lagoons (negative values). Depth and pH were significantly related to RDA2, indicating that depth

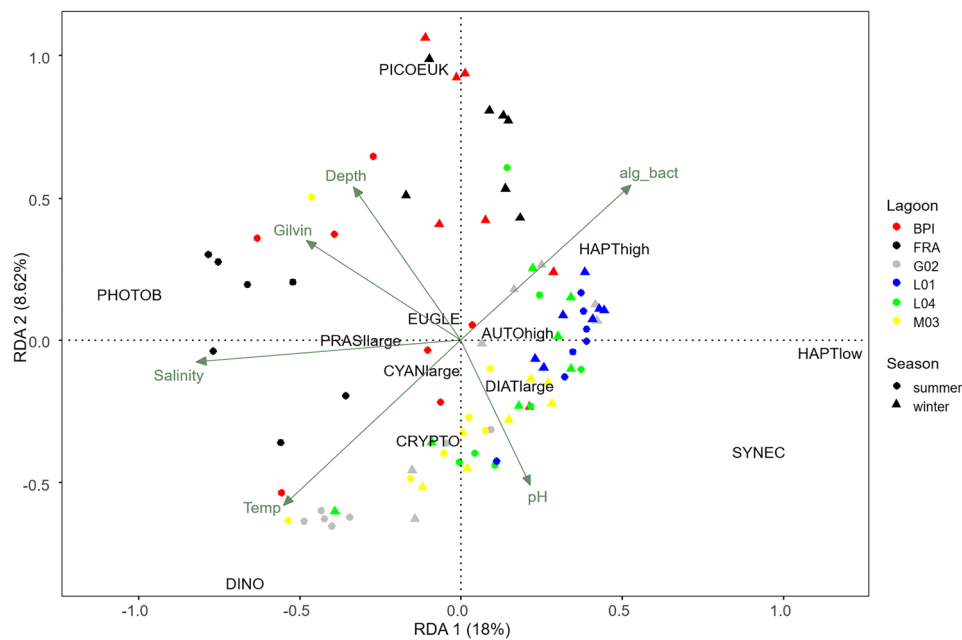


Fig. 3 Results of redundancy analysis (RDA) showing the relationships between phytoplankton composition and the first group of variables (see group 1, Table 3) for the six lagoons in La Pletera salt marsh. Only significant variables determined by a forward selection procedure are represented (in dark green). Species groups are in black. Eigenvalues (proportion explained as a percentage) of the first two axes are shown in parentheses on the corresponding axes. Monthly samples were assigned to one of two different sea-

sons: summer (May–September) and winter (October–April). *EUGLE* euglenophytes, *DINO* dinoflagellates, *PHOTOB* phototrophic bacteria, *HAPT* haptophytes, *SYNEC* *Synechococcus*, *PICOEUK* picoeukaryotes, *CRYPTO* cryptophytes, *alg_bact* algivorous/bacterivorous zooplankton, *CYAN* cyanobacteria, *AUTO* diatoms/prasinophytes, *DIAT* diatoms, *PRASI* prasinophytes, *low* low FL3 signal, *high* high FL3 signal, *large* identified by microscopy (color figure online)

was greater but the pH lower in natural lagoons (Figs. 3, S1). Lagoons FRA and G02 had the greatest mean depths, whereas L01 and M03 were the shallowest lagoons (Fig. 3; Table 1).

A total of 12 phytoplankton groups were identified for the six lagoons during the study period (Table 2). Temporal variations in the percentages of the different groups are shown in Fig. 4. Dinoflagellates and phototrophic bacteria dominated during confinement conditions (negative values, RDA1), with the latter only in natural lagoons (especially in FRA) and the former mainly in artificial lagoons (Figs. 3, 4). Haptophytes (*Pavlova*-like cells and *Prymnesium*-like cells) and *Synechococcus* dominated during flooding conditions (positive values, RDA1) in artificial lagoons (Figs. 3, 4). Picoeukaryotes were mainly dominant in the natural lagoons (positive values, RDA2) during the flooding period, while cryptophytes were more frequent in artificial ones (Figs. 3, 4). The other phytoplankton groups appeared in a central position in the RDA plot. Overall, the phytoplankton compositions in the artificial lagoons were characterised by the presence of a higher number of motile and phagotrophic species that belong to groups including potentially harmful species, while the natural lagoons were dominated by small-sized, strictly autotrophic picoeukaryotes (Figs. 3, 4 and S4).

Regarding metabolic rates, higher GPP and ER were recorded during the summer, although both showed high variability during this season (Fig. S4). Thus, GPP and ER had low correlations with RDA1, and in opposite directions, with higher ER rates during confinement (Figs. 5, S1). Rates of GPP and ER standardized to temperature, and also to light for GPP, as well as ER_TOC and GPP_chla, were positively related to RDA1 (Fig. 5), so an increase in their values under flooding conditions, especially GPP_{20MAX} and GPP_chla, indicated a higher capacity for production and a higher productivity/biomass (P/B) ratio during these conditions. In contrast, the ratio used as a proxy of the *K-r* gradient (GPP_{MAX-A}) was negatively correlated with RDA1 (Figs. 5 and S1), which suggested a higher dominance of *K* species under confinement conditions. Finally, the vector position of all these productivity-related variables indicated a low relationship with RDA2, indicating that metabolic processes did not particularly differ according to the origin of the lagoons (Figs. 5, S1).

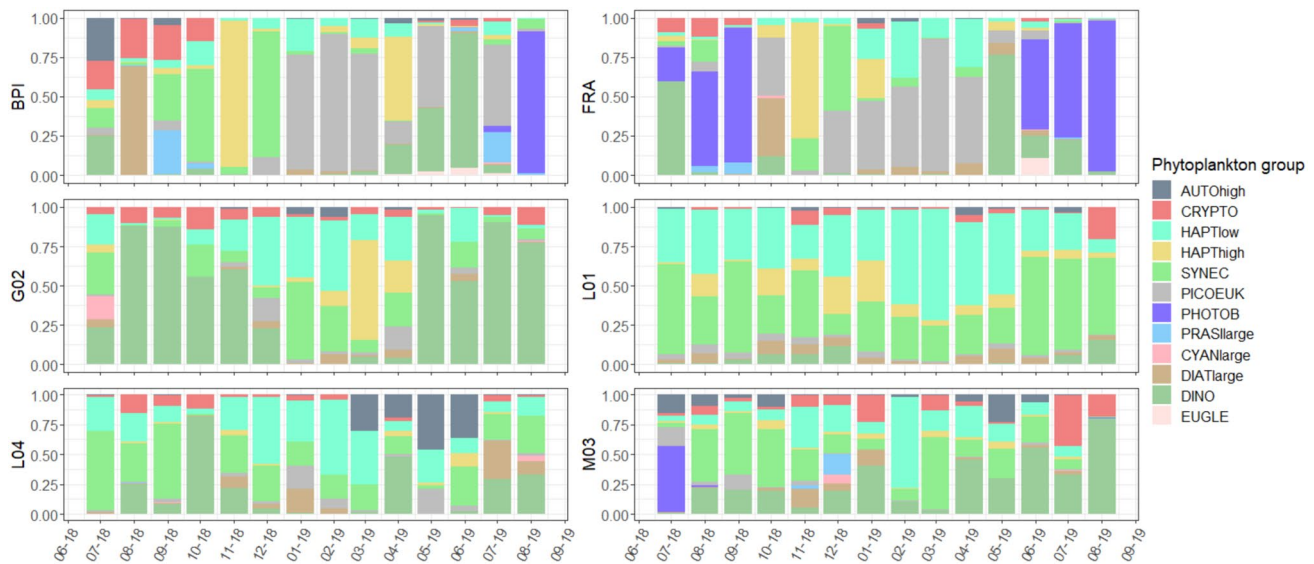
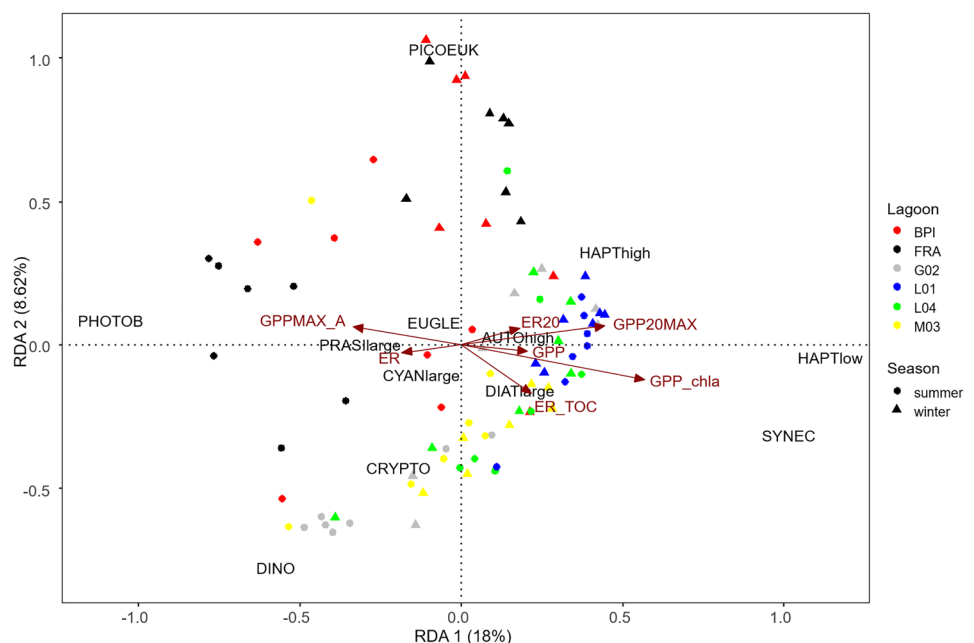


Fig. 4 Temporal changes in the biovolume ($\mu\text{m}^3/\text{mL}$) of phytoplankton groups, expressed as percentages, for the natural (BPI and FRA) and artificial lagoons (G02, L01, L04, M03) of La Pletera salt marsh.

The x-axis labels indicate the month [January–December (01–12)] and year [2018 (18) and 2019 (19)]. For abbreviations meanings, see Fig. 3; for details of the groups' characteristics, see Table 2

Fig. 5 Results of RDA between phytoplankton composition and productivity-related variables included as supplementary variables (in red; group 2, Table 3) for the six lagoons in La Pletera salt marsh. Species groups are indicated in black. Eigenvalues (proportion explained as a percentage) of the first two axes are expressed in parentheses on the corresponding axes. Monthly samples were assigned to one of two different seasons: summer (May–September) and winter (October–April). *GPP20MAX* GPP standardized to 20 °C and maximum light, *ER_TOC* ER/total organic carbon, *GPP_chla* GPP/chorophyll a; for other abbreviations, see Fig. 3; for details of the species groups' characteristics, see Tables 2, 3 (color figure online)



Discussion

Phytoplankton composition in confined coastal lagoons

The main factor accounting for differences in phytoplankton composition was season, as a result of the flooding-confinement patterns in winter and summer, which has also been previously described for this type of salt marsh

(Quintana and Moreno-Amich 2002; López-Flores et al. 2006a, 2009). This seasonal pattern is characterised by changes in water inputs and salinity, with flooding events occurring mainly in the winter followed by a dramatic decrease in water level and increase in salinity due to evaporation during the summer (Badosa et al. 2006; López-Flores et al. 2006a; Menció et al. 2017). The phytoplankton composition of natural lagoons was discriminated from that of artificial ones by the RDA analysis. The natural lagoons BPI and FRA are characterized by higher

concentrations of nutrients and organic matter than the artificial lagoons (Badosa et al. 2006; Cabrera et al. 2019), as a consequence of the progressive accumulation of these during successive flooding-confinement processes. Thus, differences in phytoplankton composition between the natural and artificial lagoons could be related to differences in nutrient availability. Moreover, higher variation in oxygen levels and metabolism have already been described for the two natural lagoons during summer, a period that was characterized by extended periods of anoxia that could last several days, in which percentage DO was lower than 5% (Bas-Silvestre et al. 2020). Overall, our results agree with those of previous studies on coastal lagoons that noted seasonality (Cañavate et al. 2015; Coelho et al. 2015), as well as salinity, temperature, transparency and nutrients, as the most important factors determining changes in the phytoplankton community (López-Flores et al. 2014; Cañavate et al. 2015; Hemraj et al. 2017; Pulina et al. 2018). In the present study, physical changes, represented by the flooding-confinement pattern, and the differences in nutrient availability between the natural and newly created lagoons, could be easily related to the two main axes of Margalef's mandala (Margalef 1978).

The main, dominant phytoplankton groups in La Pletera can be explained by the adaptation of their component species to the specific ecological characteristics of these confined Mediterranean coastal lagoons. BPI and FRA have summer blooms of phototrophic bacteria as a consequence of oxygen depletion even in surface waters. This type of situation has been described in coastal lagoons with extremely high organic matter concentrations (Madigan and Jung 2009; Fontes et al. 2011; Lamy et al. 2011). Dinoflagellates are abundant in BPI and FRA, and are known to be dominant under stable conditions of maximum confinement, when nutrients are mostly present in organic forms (López-Flores et al. 2006b; Vandersea et al. 2018; Jiang et al. 2019). Smaller picoplankton, which abound during the winter (flooding period), are under high predatory pressure from calanoid grazers, which are dominant during this season (Cabrera et al. 2019), probably because of high growth rates (Witt et al. 1981; Bec et al. 2008 and references therein). The small size of the phytoplankton [picoeukaryotes, haptophytes (*Pavlova*-like cells, *Prymnesium*-like cells)] and the scarcity of seagrasses in these two natural lagoons could indicate that the transfer of energy and carbon is less efficient in them than in the artificial lagoons due to their more complex food webs (Pulina et al. 2018). In the artificial lagoons, nitrogen-fixing cyanobacteria and potential phagotrophic haptophytes (*Pavlova*-like cells and *Prymnesium*-like cells) were more abundant, probably as a result of the lower availability of nutrients, and especially that of inorganic nitrogen forms. Phagotrophy or atmospheric nitrogen fixation are common nitrogen uptake mechanisms

in Mediterranean confined salt marshes, where an imbalance in the N/P ratio, specifically the $\text{NO}_3^-/\text{PO}_4^{3-}$ ratio, is the rule rather than the exception thanks to faster rates of denitrification than of nitrification (Quintana et al. 1998; Quintana and Moreno-Amich 2002; López-Flores et al. 2014). Strictly autotrophic, non-N fixers and *Nannochloris*-like picoeukaryotes mainly appear in natural lagoons, which are richer in organic matter, the decomposition of which might provide ammonium as a source of inorganic nitrogen (Sunda and Hardison 2007; Glibert 2016; Schulien et al. 2017). Smaller picoplankton represent a high percentage of the phytoplankton biomass. Although previously considered important groups in oligotrophic waters, they have been increasingly reported in brackish and eutrophic environments (Paoli et al. 2007; Pulina et al. 2012, 2018). Other strictly autotrophic nano- and microphytoplankton, such as diatoms and chlorophytes, are generally rare in this type of salt marsh, as their growth is limited by the lack of inorganic nitrogen (Quintana and Moreno-Amich 2002).

Productivity-related variables

Ecosystem metabolism estimations have rarely been applied in community composition studies (e.g. Murrell et al. 2018), yet DO sensors, as used in the present study, provide data for GPP and ER estimation that could be used in our multivariate species composition analysis to better elucidate patterns in the species composition of phytoplankton. Furthermore, terms such as 'productivity', although frequently used in the literature in studies on phytoplankton, are generally used conceptually and rarely refer to measured variables (López-Flores et al. 2006a; Pulina et al. 2012, 2017). Metabolic rates can also be combined with other biomass approximations, such as the total amount of chlorophyll *a*, to obtain a quantifiable proxy for the P/B ratio, which is a term with important connotations for ecology, but again, is sometimes only used conceptually.

When the productivity-related variables were included in the RDA, they generally showed a positive correlation with the first RDA axis, which is related to seasonal changes in physical variables. This was not only seen for metabolic rates but also for the standardized rates and GPP_chl*a* ratio. These findings agree with the general ecological theory that the P/B ratio should decrease with succession, or in the case of phytoplankton, with seasonal succession (Margalef 1968, 1978; Odum and Barrett 1971), which suggests that these types of ratios can be helpful proxies for productivity. However, they should be used in this way with caution, since metabolic rates derived from diel DO changes not only relate to production from phytoplankton but also to that from all other primary producers of the ecosystem. Seagrasses, macroalgae, biofilms and periphyton also contribute to total lagoon GPP, thus high production in a water body

does not necessarily entirely correspond to phytoplankton metabolism. In any case, we found a significant relationship between phytoplankton GPP and DO even in our lagoons, which are shallow and where the relative importance of benthic metabolism is potentially high (e.g. see MacIntyre et al. 1996; McGlathery et al. 2001). Therefore, we can assume that the relationship between DO and GPP would be even stronger in exclusively planktonic open waters, where GPP is determined by that of phytoplankton.

The BASE model, which was used to calculate the metabolic rates (Grace et al. 2015; Giling et al. 2017; Bas-Silvestre et al. 2020) in the present study gave an interesting result. Some of the ecophysiological parameters derived from the ecosystem metabolism estimation methods can be effectively applied from a community structure perspective. One example of this is the GPP_{MAX_A} ratio used here (see “Materials and methods”), which provides a proxy for the relative importance of the *K*- and *r*-strategies, concepts widely used in ecology but rarely quantified. In the present study, GPP_{MAX_A} lined up with the first RDA axis, suggesting a gradual change from a *K*- to a *r*-strategy related to the physical flooding-confinement gradient, in agreement with a progressive increase in *K*-strategists during seasonal succession. Thus, automated oxygen sensors could provide a high-frequency, easy-to-obtain proxy for the relative importance of *K*- and *r*-strategies in the aquatic communities of the lagoons studied here. However, once again, some issues should be taken into consideration, some of which are related to the particularities of confined coastal lagoons because the flooding-confinement pattern represents the main seasonal gradient and, therefore, the main gradient of stability, although other, short-term, low-intensity disturbances (storm events of short duration, windy or rainy days) may also affect the proportions of *r*- and *K*-strategists. Moreover, high accumulation of organic matter under maximum confinement may lead to anoxic conditions (Bas-Silvestre et al. 2020), which are far from stable conditions. Other potential issues might have a theoretical basis because the relationship between P-I curves and growth model parameters can only be assessed under certain assumptions: steady-state photosynthesis rates, photosynthesis rates adapted to growth irradiance, zero maintenance costs and fixed carbon:cell and chlorophyll:biomass ratios (Cullen 1990; Zonneveld 1998; Litchman and Klausmeier 2008). However, none of these assumptions are actually true under natural conditions.

In conclusion, estimations of metabolic rates can provide measurable parameters of species composition when ecosystem metabolism is combined with community structure studies. We propose the use of the GPP_chl_a ratio as an estimation of the P/B ratio, and the GPP_{MAX_A} ratio as a proxy for the relative importance of *K*- and *r*-strategists. Using these ratios, a decrease in the P/B ratio and prevalence of *K*-strategists with seasonal succession, as predicted by Margalef’s

mandala, has been observed. A better understanding of ecosystem functioning could provide new insights into how aquatic ecosystems, and more specifically highly variable coastal lagoons, will respond to changes in their physical and chemical characteristics, and planktonic assemblages, with global change.

Supplementary Information The online version contains supplementary material available at <https://doi.org/10.1007/s00027-024-01084-9>.

Acknowledgements The authors are grateful to all of the people who contributed to the fieldwork, and especially to Mònica Martinoy and Josep Pascual, who provided supporting data, such as water levels, salinity values and density profiles of La Pletera lagoons, as well as meteorological data of the study area. This work was supported by the LIFE+ Program of the European Commission (LIFE Pletera; LIFE13NAT/ES/001001); the Ministerio de Economía y Competitividad (CGL 2016-76024-R AEI/FEDER/UE); by grant PID2020-114440GB-I00 funded by MCIN/AEI/10.13039/501100011033, from the European Union’s Horizon 2020 research and innovation programme under grant agreement No. 869296—The PONDERFUL project; the Generalitat de Catalunya (2017 SGR 548); and the University of Girona (IFUG 2017).

Author contributions Conceptualization: M.B.-S., M.A.-P., D.B., S.G., J.C., B.O. and X.D.Q. Data curation, formal analysis, validation, methodology and visualization: M.B.-S.; investigation: M.B.-S., M.A.-P., D.B., J.B. and X.D.Q. Funding acquisition, project administration, resources and supervision: X.D.Q.. Writing—original draft: M.B.-S.. Writing—review and editing: all authors.

Funding Open Access funding provided thanks to the CRUE-CSIC agreement with Springer Nature. This article is funded by the LIFE programme, LIFE13NAT/ES/001001, Ministerio de Economía y Competitividad, CGL 2016-76024-R AEI/FEDER/UE, Generalitat de Catalunya, 2017 SGR 548, Universitat de Girona, IFUG 2017, MCIN/AEI/10.13039/501100011033, PID2020-114440 GB-I00. Also, part of this research has received funding from the European Union’s Horizon 2020 research and innovation programme under grant agreement No 869296 – The PONDERFUL Project.

Data availability The datasets generated during and/or analyzed during the current study are available from the corresponding author on reasonable request.

Declarations

Conflict of interest The authors have no conflicts of interest to declare that are relevant to the content of this article.

Open Access This article is licensed under a Creative Commons Attribution 4.0 International License, which permits use, sharing, adaptation, distribution and reproduction in any medium or format, as long as you give appropriate credit to the original author(s) and the source, provide a link to the Creative Commons licence, and indicate if changes were made. The images or other third party material in this article are included in the article’s Creative Commons licence, unless indicated otherwise in a credit line to the material. If material is not included in the article’s Creative Commons licence and your intended use is not permitted by statutory regulation or exceeds the permitted use, you will need to obtain permission directly from the copyright holder. To view a copy of this licence, visit <http://creativecommons.org/licenses/by/4.0/>.

References

- APHA (2005) Standard methods for the examination of water and wastewater, 21st edn. American Public Health Association, American Water Works Association and Water Environment Federation, Washington, DC
- Badosa A, Boix D, Brucet S et al (2006) Nutrients and zooplankton composition and dynamics in relation to the hydrological pattern in a confined Mediterranean salt marsh (NE Iberian Peninsula). *Estuar Coast Shelf Sci* 66:513–522. <https://doi.org/10.1016/j.ecss.2005.10.006>
- Balch WM (2004) Re-evaluation of the physiological ecology of coccolithophores. In: Thiersten HR, Young JR (eds) *Coccolithophores—from molecular processes to global impact*. Springer, Berlin, Heidelberg, New York pp 165–190
- Bas-Silvestre M, Quintana XD, Compte J et al (2020) Ecosystem metabolism dynamics and environmental drivers in Mediterranean confined coastal lagoons. *Estuar Coast Shelf Sci* 245:106989. <https://doi.org/10.1016/j.ecss.2020.106989>
- Bec B, Collos Y, Vaquer A et al (2008) Growth rate peaks at intermediate cell size in marine photosynthetic picoeukaryotes. *Limnol Oceanogr* 53:863–867. <https://doi.org/10.4319/lo.2008.53.2.0863>
- Brito AC, Newton A, Tett P, Fernandes TF (2012) How will shallow coastal lagoons respond to climate change? A modelling investigation. *Estuar Coast Shelf Sci* 112:98–104. <https://doi.org/10.1016/J.ECSS.2011.09.002>
- Cabrera S, Compte J, Gascón S et al (2019) How do zooplankton respond to coastal wetland restoration? the case of newly created salt marsh lagoons in La Pletera (NE Catalonia). *Limnetica* 38:721–741. <https://doi.org/10.23818/limn.38.42>
- Cañavate JP, Pérez-Gavilan C, Mazuelos N, Machado M (2015) Flushing-related changes of phytoplankton seasonal assemblages in marsh ponds of the warm temperate Guadalquivir river estuary (SW Spain). *Hydrobiologia* 744:15–33. <https://doi.org/10.1007/s10750-014-2051-x>
- Coelho S, Pérez-Ruzafa A, Gamito S (2015) Phytoplankton community dynamics in an intermittently open hypereutrophic coastal lagoon in southern Portugal. *Estuar Coast Shelf Sci* 167:102–112. <https://doi.org/10.1016/j.ecss.2015.07.022>
- Cullen JJ (1990) On models of growth and photosynthesis in phytoplankton. *Deep Sea Res Part A Oceanogr Res Papers* 37:667–683. [https://doi.org/10.1016/0198-0149\(90\)90097-F](https://doi.org/10.1016/0198-0149(90)90097-F)
- Cullen JJ, Franks PJS, Karl DM, Longhurst A (2002) Physical influences on marine ecosystem dynamics. In: Robinson AR, McCarthy JJ, Rothschild BJ (eds) *The sea: biological-physical interactions in the ocean*. Wiley, New York, pp 297–335
- Cullen JJ, Ford Doolittle W, Levin SA, Li WKW (2007) Patterns and prediction in microbial oceanography. *Oceanography* 20:34–46. <https://doi.org/10.5670/oceanog.2007.46>
- Derolez V, Soudant D, Malet N et al (2020) Two decades of oligotrophication: evidence for a phytoplankton community shift in the coastal lagoon of Thau (Mediterranean Sea, France). *Estuar Coast Shelf Sci* 241:106810. <https://doi.org/10.1016/j.ecss.2020.106810>
- Duarte P, Macedo MF, da Fonseca LC (2006) The relationship between phytoplankton diversity and community function in a coastal lagoon. In: Queiroga H, Cunha MR, Cunha A et al (eds) *Marine biodiversity: patterns and processes, assessment, threats, management and conservation*. Springer, Dordrecht, pp 3–18
- Einsle U (1993) *Crustacea, Copepoda, Calanoida und Cyclopoida—Süsswasserfauna von Mitteleuropa*. Fischer, Stuttgart
- Esri (2020) ArcGIS Pro (Version 2.5). Esri
- Flynn KJ, Stoecker DK, Mitra A et al (2013) Misuse of the phytoplankton–zooplankton dichotomy: the need to assign organisms as mixotrophs within plankton functional types. *J Plankton Res* 35:3–11. <https://doi.org/10.1093/plankt/fbs062>
- Fontes MLS, Suzuki MT, Cottrell MT, Abreu PC (2011) Primary production in a subtropical stratified coastal lagoon—contribution of anoxygenic phototrophic bacteria. *Microb Ecol* 61:223–237. <https://doi.org/10.1007/s00248-010-9739-x>
- Gaedke U (1992) The size distribution of plankton biomass in a large lake and its seasonal variability. *Limnol Oceanogr* 37:1202–1220. <https://doi.org/10.4319/lo.1992.37.6.1202>
- Gasol JM, Morán XAG (2015) Flow cytometric determination of microbial abundances and its use to obtain indices of community structure and relative activity. In: McGenity T, Timmis K, Nogales B (eds) *Hydrocarbon and lipid microbiology protocols*. Springer, Berlin, Heidelberg, New York, pp 159–187
- Giling DP, Staehr PA, Grossart HP et al (2017) Delving deeper: metabolic processes in the metalimnion of stratified lakes. *Limnol Oceanogr* 62:1288–1306. <https://doi.org/10.1002/lno.10504>
- Glibert PM (2016) Margalef revisited: a new phytoplankton mandala incorporating twelve dimensions, including nutritional physiology. *Harmful Algae* 55:25–30. <https://doi.org/10.1016/j.hal.2016.01.008>
- Grace MR, Giling DP, Hladysz S et al (2015) Fast processing of diel oxygen curves: estimating stream metabolism with BASE (Bayesian Single-station Estimation). *Limnol Oceanogr Methods* 13:e10011. <https://doi.org/10.1002/lom3.10011>
- Grasshoff K, Kremling K, Ehrhardt M (1999) *Methods of seawater analysis*. Wiley-VCH, Weinheim
- Hemraj DA, Hossain MA, Ye Q et al (2017) Plankton bioindicators of environmental conditions in coastal lagoons. *Estuar Coast Shelf Sci* 184:102–114. <https://doi.org/10.1016/j.ecss.2016.10.045>
- Hillebrand H, Dürselen C-D, Kirschtel D et al (1999) Biovolume calculation for pelagic and benthic microalgae. *J Phycol* 35:403–424. <https://doi.org/10.1046/j.1529-8817.1999.3520403.x>
- Hoellein TJ, Bruesewitz DA, Richardson DC (2013) Revisiting Odum (1956): a synthesis of aquatic ecosystem metabolism. *Limnol Oceanogr* 58:2089–2100. <https://doi.org/10.4319/lo.2013.58.6.2089>
- Jakubowska N, Szlag-Wasielewska E (2015) Toxic picoplanktonic cyanobacteria—review. *Mar Drugs* 13:1497–1518. <https://doi.org/10.3390/md13031497>
- Jeffrey SW, Mantoura RF, Wright SW (eds) (1997) *Phytoplankton pigments in oceanography: guidelines to modern methods*. UNESCO, Paris
- Jiang Z, Chen J, Gao Y et al (2019) Regulation of spatial changes in phytoplankton community by water column stability and nutrients in the Southern Yellow Sea. *J Geophys Res Biogeosci* 124:2610–2627. <https://doi.org/10.1029/2018JG004785>
- Kemp WM, Testa JM (2011) Metabolic balance between ecosystem production and consumption. In: Wolanski E, McLusky DS (eds) *Treatise on estuarine and coastal science*. Academic Press, Waltham, pp 83–118
- Kennish MJ, Paerl HW (2010) Coastal lagoons: critical habitats of environmental change. In: Kennish MJ, Paerl HW (eds) *Coastal lagoons: critical habitats of environmental change*. Taylor and Francis, Boca Raton, Francis, pp 1–17
- Kirk JTO (1994) *Light and photosynthesis in aquatic ecosystems*. Cambridge University Press, London
- Kruk C, Devercelli M, Huszar VLM (2020) Reynolds functional groups: a trait-based pathway from patterns to predictions. *Hydrobiologia* 848:113–129. <https://doi.org/10.1007/s10750-020-04340-9>
- Lamy D, Carvalho-Maalouf PD, Cottrell MT et al (2011) Seasonal dynamics of aerobic anoxygenic phototrophs in a Mediterranean coastal lagoon. *Aquat Microb Ecol* 62:153–163. https://doi.org/10.1007/978-1-4020-8815-5_1

- Legendre P, Gallagher ED (2001) Ecologically meaningful transformations for ordination of species data. *Oecologia* 129:271–280. <https://doi.org/10.1007/s004420100716>
- Leruste A, Villéger S, Malet N et al (2018) Complementarity of the multidimensional functional and the taxonomic approaches to study phytoplankton communities in three Mediterranean coastal lagoons of different trophic status. *Hydrobiologia* 815:207–227. <https://doi.org/10.1007/s10750-018-3565-4>
- Litchman E, Klausmeier CA (2008) Trait-based community ecology of phytoplankton. *Annu Rev Ecol Evol Syst* 39:615–639. <https://doi.org/10.1146/annurev.ecolsys.39.110707.173549>
- López-Flores R, Boix D, Badosa A et al (2006a) Pigment composition and size distribution of phytoplankton in a confined Mediterranean salt marsh ecosystem. *Mar Biol* 149:1313–1324. <https://doi.org/10.1007/s00227-006-0273-9>
- López-Flores R, Garcés E, Boix D et al (2006b) Comparative composition and dynamics of harmful dinoflagellates in Mediterranean salt marshes and nearby external marine waters. *Harmful Algae* 5:637–648. <https://doi.org/10.1016/j.hal.2006.01.001>
- López-Flores R, Boix D, Badosa A et al (2009) Environmental factors affecting bacterioplankton and phytoplankton dynamics in confined Mediterranean salt marshes (NE Spain). *J Exp Mar Bio Ecol* 369:118–126. <https://doi.org/10.1016/j.jembe.2008.11.003>
- López-Flores R, Quintana XD, Romaní AM et al (2014) A compositional analysis approach to phytoplankton composition in coastal Mediterranean wetlands: influence of salinity and nutrient availability. *Estuar Coast Shelf Sci* 136:72–81. <https://doi.org/10.1016/j.ecss.2013.11.015>
- MacIntyre HL, Geider RJ, Miller DC (1996) Microphytobenthos: the ecological role of the “secret garden” of unvegetated, shallow-water marine habitats. I. Distribution, abundance and primary production. *Estuaries* 19:186–201. <https://doi.org/10.2307/1352224>
- Madigan MT, Jung DO (2009) An overview of purple bacteria: systematics, physiology, and habitats. In: Hunter CN, Daldal F, Thurnauer MC, Beatty JT (eds) *The purple phototrophic bacteria*. Advances in photosynthesis and respiration. Springer, Dordrecht, pp 1–15
- Margalef R (1968) *Perspectives in ecological theory*. University of Chicago Press, Chicago
- Margalef R (1978) Life-forms of phytoplankton as survival alternatives in an unstable environment. *Oceanol Acta* 1:493–509
- McGlathery KJ, Anderson IC, Tyler AC (2001) Magnitude and variability of benthic and pelagic metabolism in a temperate coastal lagoon. *Mar Ecol Prog Ser* 216:1–15
- Menció A, Casamitjana X, Mas-Pla J et al (2017) Groundwater dependence of coastal lagoons: the case of La Pletera salt marshes (NE Catalonia). *J Hydrol* 552:793–806. <https://doi.org/10.1016/j.jhydrol.2017.07.034>
- Murrell MC, Caffrey JM, Marcovich DT et al (2018) Seasonal oxygen dynamics in a warm temperate estuary: effects of hydrologic variability on measurements of primary production, respiration, and net metabolism. *Estuaries Coasts* 41:690–707. <https://doi.org/10.1007/s12237-017-0328-9>
- Nogrady T (1993) *Rotifera*. Volume 1: biology, ecology and systematics. Guides to the identification of the microinvertebrates of the continental waters of the world. SPB, Amsterdam
- Odum HT (1956) Primary production in flowing waters. *Limnol Oceanogr* 1:102–117. <https://doi.org/10.4319/lo.1956.1.2.0102>
- Odum EP, Barrett GW (1971) *Fundamentals of ecology*. Saunders, Philadelphia
- Oksanen J, Blanchet FG, Friendly M, et al (2019) *vegan: community ecology package*. R package version 2.5-6
- Padisák J, Crosse L, Naselli-Flores L (2009) Use and misuse in the application of the phytoplankton functional classification: a critical review with updates. *Hydrobiologia* 621:1–19. <https://doi.org/10.1007/s10750-008-9645-0>
- Paoli A, Celussi M, Valeri A et al (2007) Picocyanobacteria in Adriatic transitional environments. *Estuar Coast Shelf Sci* 75:13–20. <https://doi.org/10.1016/j.ecss.2007.02.026>
- Pawlowsky-Glahn V, Buccianti A (eds) (2011) *Compositional data analysis: theory and applications*. Wiley
- Péquin B, Mohit V, Poisot T et al (2017) Wind drives microbial eukaryote communities in a temperate closed lagoon. *Aquat Microb Ecol* 78:187–200. <https://doi.org/10.3354/ame01814>
- Pérez-Ruzafa A, Pérez-Ruzafa IM, Newton A, Marcos C (2019) Coastal lagoons: environmental variability, ecosystem complexity, and goods and services uniformity. In: Wolanski E, Day JW, Elliott M, Ramachandran R (eds) *Coasts and estuaries: the future*. Elsevier, Amsterdam, pp 253–276
- Pulina S, Padedda BM, Satta CT et al (2012) Long-term phytoplankton dynamics in a Mediterranean eutrophic lagoon (Cabras Lagoon, Italy). *Plant Biosyst* 146:259–272. <https://doi.org/10.1080/11263504.2012.717545>
- Pulina S, Satta CT, Padedda BM et al (2017) Picophytoplankton seasonal dynamics and interactions with environmental variables in three Mediterranean coastal lagoons. *Estuaries Coasts* 40:469–478. <https://doi.org/10.1007/s12237-016-0154-5>
- Pulina S, Satta CT, Padedda BM et al (2018) Seasonal variations of phytoplankton size structure in relation to environmental variables in three Mediterranean shallow coastal lagoons. *Estuar Coast Shelf Sci* 212:95–104. <https://doi.org/10.1016/j.ecss.2018.07.002>
- Quintana XD, Moreno-Amich R (2002) Phytoplankton composition of Empordà salt marshes, Spain and its response to freshwater flux regulation. *J Coast Res* 36:581–590. <https://doi.org/10.2112/1551-5036-36.sp1.581>
- Quintana XD, Moreno-Amich R, Comín FA (1998) Nutrient and plankton dynamics in a Mediterranean salt marsh dominated by incidents of flooding. Part 1. Differential confinement of nutrients. *J Plankton Res* 20:2089–2107. <https://doi.org/10.1093/plankt/20.11.2089>
- Quintana XD, Boix D, Casamitjana X, et al (2018) Management and restoration actions of confined Mediterranean coastal lagoons in the Empordà and Baix Ter Wetlands. In: Quintana XD, Boix D, Gascón S, Sala J (eds) *Management and restoration of Mediterranean coastal lagoons in Europe*. Càtedra d’Ecosistemes Litorals Mediterranis, Torroella de Montgrí, pp 173–192
- Quintana XD, Antón-Pardo M, Bas-Silvestre M et al (2021) Identifying critical transitions in seasonal shifts of zooplankton composition in a confined coastal salt marsh. *Aquat Sci* 83:1–17. <https://doi.org/10.1007/S00027-021-00824-5>
- R Core Team (2017) *R: a language and environment for statistical computing*. <http://www.R-project.org/>. R Foundation for Statistical Computing, Vienna, Austria
- Reynolds CS (2006) *The ecology of phytoplankton*. Cambridge University Press, Cambridge
- Saccà A (2016) Confined coastal lagoons: extraordinary habitats at risk. In: Snyder C (ed) *Coastal lagoons: geology, characteristics and diversity*. Nova, Hauppauge, New York, pp 1–21
- Schulien JA, Peacock MB, Hayashi K et al (2017) Phytoplankton and microbial abundance and bloom dynamics in the upwelling shadow of Monterey Bay, California, from 2006 to 2013. *Mar Ecol Prog Ser* 572:43–56. <https://doi.org/10.3354/meps12142>
- Seoane S, Garmendia M, Revilla M et al (2011) Phytoplankton pigments and epifluorescence microscopy as tools for ecological status assessment in coastal and estuarine waters, within the water framework directive. *Mar Pollut Bull* 62:1484–1497. <https://doi.org/10.1016/j.marpolbul.2011.04.010>
- Staehr PA, Bade DL, Van de Bogert MC et al (2010) Lake metabolism and the diel oxygen technique: state of the science. *Limnol Oceanogr Methods* 8:628–644. <https://doi.org/10.4319/lom.2010.8.0628>

- Staehr PA, Testa JM, Kemp WM et al (2012) The metabolism of aquatic ecosystems : history, applications, and future challenges. *Aquat Sci* 74:15–29. <https://doi.org/10.1007/s00027-011-0199-2>
- Stoecker DK, Hansen PJ, Caron DA, Mitra A (2017) Mixotrophy in the marine plankton. *Ann Rev Mar Sci* 9:311–335. <https://doi.org/10.1146/annurev-marine-010816-060617>
- Sunda WG, Hardison DR (2007) Ammonium uptake and growth limitation in marine phytoplankton. *Limnol Oceanogr* 52:2496–2506. <https://doi.org/10.4319/lo.2007.52.6.2496>
- Trobajo R, Quintana XD, Moreno-Amich R (2002) Model of alternative predominance of phytoplankton-periphyton-macrophytes in lentic waters of Mediterranean coastal wetlands. *Arch Hydrobiol* 154:19–40. <https://doi.org/10.1127/archiv-hydrobiol/154/2002/19>
- Utermöhl H (1958) Zur Vervollkommnung der quantitativen Phytoplankton-Methodik. *Mitt Int Ver Theor Angew Limnol* 9:1–38
- Vandersea MW, Kibler SR, Tester PA et al (2018) Environmental factors influencing the distribution and abundance of *Alexandrium catenella* in Kachemak Bay and Lower Cook Inlet, Alaska. *Harmful Algae* 77:81–92. <https://doi.org/10.1016/j.hal.2018.06.008>
- Villamaña M, Marañón E, Cermeño P et al (2019) The role of mixing in controlling resource availability and phytoplankton community composition. *Prog Oceanogr* 178:102181. <https://doi.org/10.1016/j.pocean.2019.102181>
- Wickham H (2016) *ggplot2: Elegant Graphics for Data Analysis*. Springer, Cham
- Witt U, Koske PH, Kuhlmann D et al (1981) Production of *Nannochloris* sp. (Chlorophyceae) in large-scale outdoor tanks and its use as a food organism in marine aquaculture. *Aquaculture* 23:171–181. [https://doi.org/10.1016/0044-8486\(81\)90012-0](https://doi.org/10.1016/0044-8486(81)90012-0)
- Zapata M, Rodríguez F, Garrido JL (2000) Separation of chlorophylls and carotenoids from marine phytoplankton: a new HPLC method using a reverse phase C8 column and pyridine-containing mobile phases. *Mar Ecol Prog Ser* 195:29–45. <https://doi.org/10.3354/meps195029>
- Zonneveld C (1998) Light-limited microalgal growth: a comparison of modelling approaches. *Ecol Modell* 113:41–54. [https://doi.org/10.1016/S0304-3800\(98\)00133-1](https://doi.org/10.1016/S0304-3800(98)00133-1)
- Zwart JA, Solomon CT, Jones SE (2015) Phytoplankton traits predict ecosystem function in a global set of lakes. *Ecology* 96:2257–2264. <https://doi.org/10.1890/14-2102.1>

Publisher's Note Springer Nature remains neutral with regard to jurisdictional claims in published maps and institutional affiliations.